



Embedded Design Techniques for Optimizing Control Parameters

Introduction

In the process of optimizing control functions, small adjustments in microcontroller firmware can produce significant improvements in embedded system performance. Coming up with the right values for gains, offsets, delays, hysteresis values and PWM parameters can be time consuming, but using the right tools can speed the process.

While it's possible to optimize control systems through calculation and modeling, today's design tools enable faster real-world measurements and simpler determination of optimal design settings. Flash memory, flexible development environments, and the capabilities of modern deep-memory, mixed signal oscilloscopes to monitor many points simultaneously, combine to form a powerful solution toolkit.

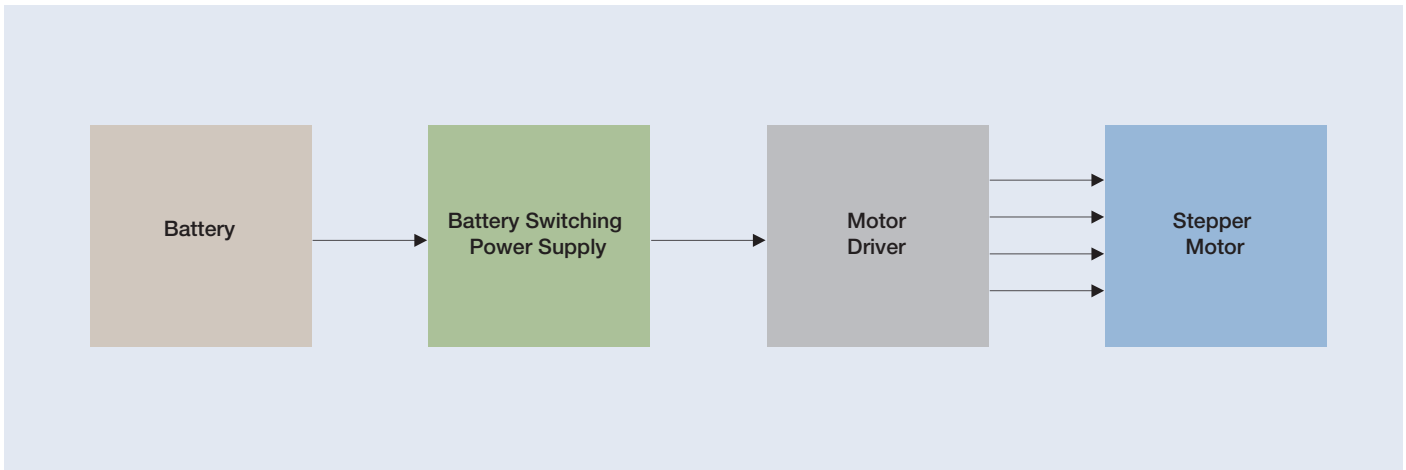


Figure 1.1. Block diagram of motor drive.

Real-time control applications demand precise interaction of firmware algorithms, analog sensors and feedback mechanisms. Traditional four-channel oscilloscopes quickly run out of channels and limit your ability to effectively analyze your design. With a mixed signal oscilloscope, especially one with deep memory, you efficiently gain access to insights of your process including sensor signals, feedback signals and firmware timing.

This application note covers three actual applications in which specific measurement techniques were used to quickly optimize key control parameters in microcontroller-based systems.

Application 1. Battery Powered Stepper Motor Control with Switching Power Supply

In this application example we will look at a low power stepper motor driven from a single Lithium cell. The cell voltage is stepped up from a nominal 2.5 Volts with a boost power converter. There are two challenges in this application. One is that the battery has a limited average current capability of 120 mA. The other is that the voltage from the boost

converter sags when high current is drawn. The average current drawn by the stepper motor can be reduced by putting a delay between steps in the motor drive. There is also some quiescent current consumption. This means that the total energy consumed during the movement of the motor increases as the motor is operated more slowly. Figure 1.1 shows a block diagram of the system.

The objective in this application is to determine the most efficient operating mode for the motor drive considering the current drawn and the quiescent operating power while also limiting the battery current to a safe level for the battery. We also need to identify an even lower current mode in which the battery current is limited to 60 mA for when the battery is near the end of its life.

In this example, we will be taking advantage of the deep memory of the MSO4000 Series mixed signal oscilloscope to take data at several operating conditions at once. We will use the measurement capability to measure voltages and currents over specific intervals by using the cursors and setting the measurements to provide information based on the sections of the waveforms between the cursors. The cursors will also provide time measurements between specific events.

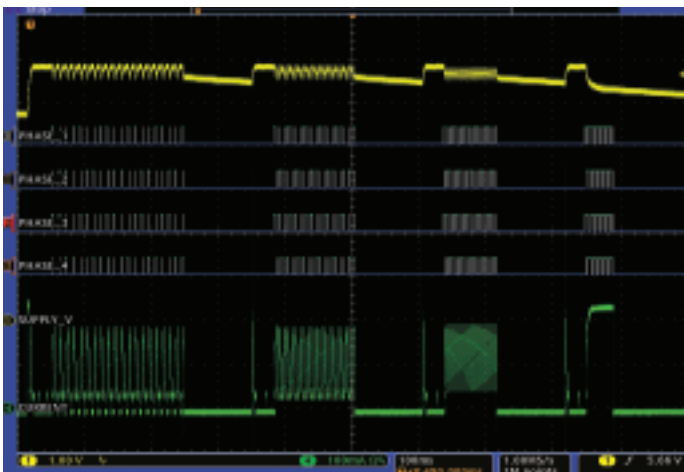


Figure 1.2. Capture with four different motor step delays.

Figure 1.2 shows the capture in which 4 different delays between the motor steps were tried. Delays of 2, 4 and 8 milliseconds were tested, in addition to no delay, to cover a wide range of delay conditions. We can extrapolate between these settings, and run additional tests to confirm the final numbers if needed. The yellow trace labeled “SUPPLY_V” shows the power supply voltage. It is a nominal 6 Volt supply, but it sags under the load from the motor. The green trace labeled “CURRENT” shows the battery current. This was measured with a Tektronix current probe in the line from the battery to the power supply. The four phase lines of the stepper motor are shown as digital lines labeled “PHASE_1” to “PHASE_4”. Since this is a low voltage motor, the motor voltage can be applied directly to the digital lines of the oscilloscope. Having the motor signals assures that the motor phases are being driven correctly. While analog signals would have been desirable, few oscilloscopes have more than 4 analog channels available, and the digital signals adequately provide the timing information about the motor operation.



Figure 1.3. No delay between steps.

From Figure 1.2, it is clear that the current over the time period is highest for the motor operation toward the right side of the trace, but that this takes the shortest period. The energy used from the battery can be expressed in milliamps x milliseconds; that is the current multiplied by the time. Thus, a lower current for a longer period of time may use more of the battery energy than a higher current for a shorter time. For the four sections of the capture, we will look at the average current and the time to identify the best operating point. Of course the maximum operating current of the battery is a key factor in the decision of which delay to use.

In the lower portion of Figure 1.3, the display is zoomed in on the time where the motor is operated with no delay between motor steps. The zoomed area of the acquired waveforms are shown with the gray brackets in the upper right corner of the display. The average current during the time for the 20 steps of the motor is 224 mA over a period of 42 milliseconds for a total energy of 9408 mA * ms. The voltage drops to 5.20 Volts, which is below the optimal voltage for the motor. The battery current is much higher than the 120 mA limit.

In Figure 1.4, a 2 millisecond delay is introduced between each step. Here the average current is only 132 mA, but for a period of 80 milliseconds for a total energy of 10,560 mA * ms. The energy consumed is higher, but the maximum current is lower. The voltage at the end the motor motion period at 5.48 Volts is significantly higher than in the first case with no delay. The average current is close to the desired level, but is still too high.

In Figure 1.5, the delay between steps is extended to 4 milliseconds between motor steps. Here the average current is only 93 mA, but for a period of 120 milliseconds for a total energy of 11160 mA * ms. The energy consumed is even higher than the last example, but the maximum current is lower. The Voltage ends the motor motion period at the same 5.48 Volts as in Figure 1.4, which has the 2 millisecond delay between pulses. We can see that the current with 2 milliseconds between pulses is too high, but the current with a 4 millisecond delay is substantially lower than the specification of 120 mA of battery current. It appears than a 3 millisecond delay will be the best compromise using less energy than a 4 millisecond delay, but having the battery current comfortably below the limit.

We still need to find the delay for use when the battery is nearly depleted and can only provide 60 mA. Figure 1.6 shows the waveform and measurements with an 8 millisecond delay between motor steps. Here the average current is only 57 mA, but for a period of 200 milliseconds for a total energy of 11400 mA * ms. The energy is a little higher than in Figure 1.5, but the current is now below the level we need for a depleted battery. The voltage at the end of the motor movement is unchanged and is acceptable.

We have used the long record length and the measurement capabilities of the oscilloscope to quickly determine the best operating points for a complex stepper motor and voltage regulator system. Only one scope capture was needed, and the measurements were made of the various operating conditions by moving the cursors. The ability to measure waveform parameters between cursors was key to being able to quickly make this design decision. Capturing the motor phase drive signals allowed confirming the time between motor steps as well as confirming the correct operation of the motor.



Figure 1.4. Two millisecond delay between steps.

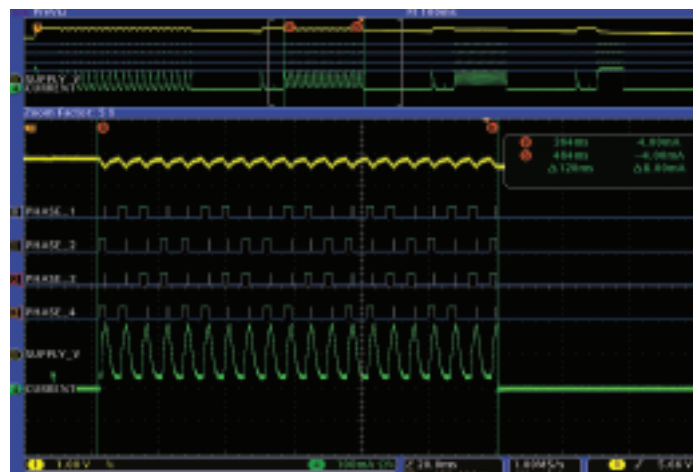


Figure 1.5. Four millisecond delay between steps.

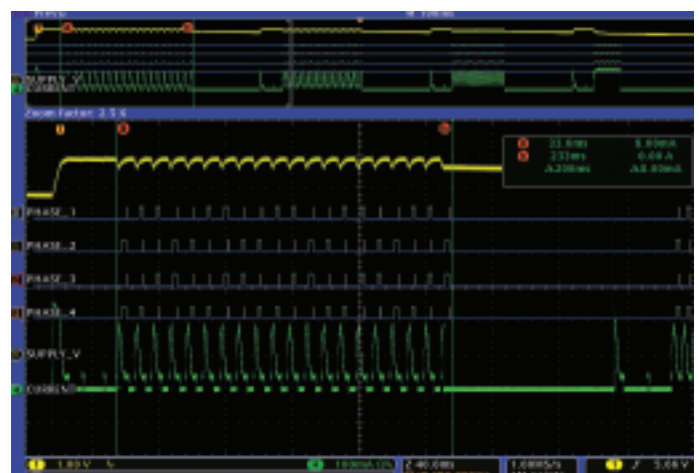


Figure 1.6. Eight millisecond delay between steps.

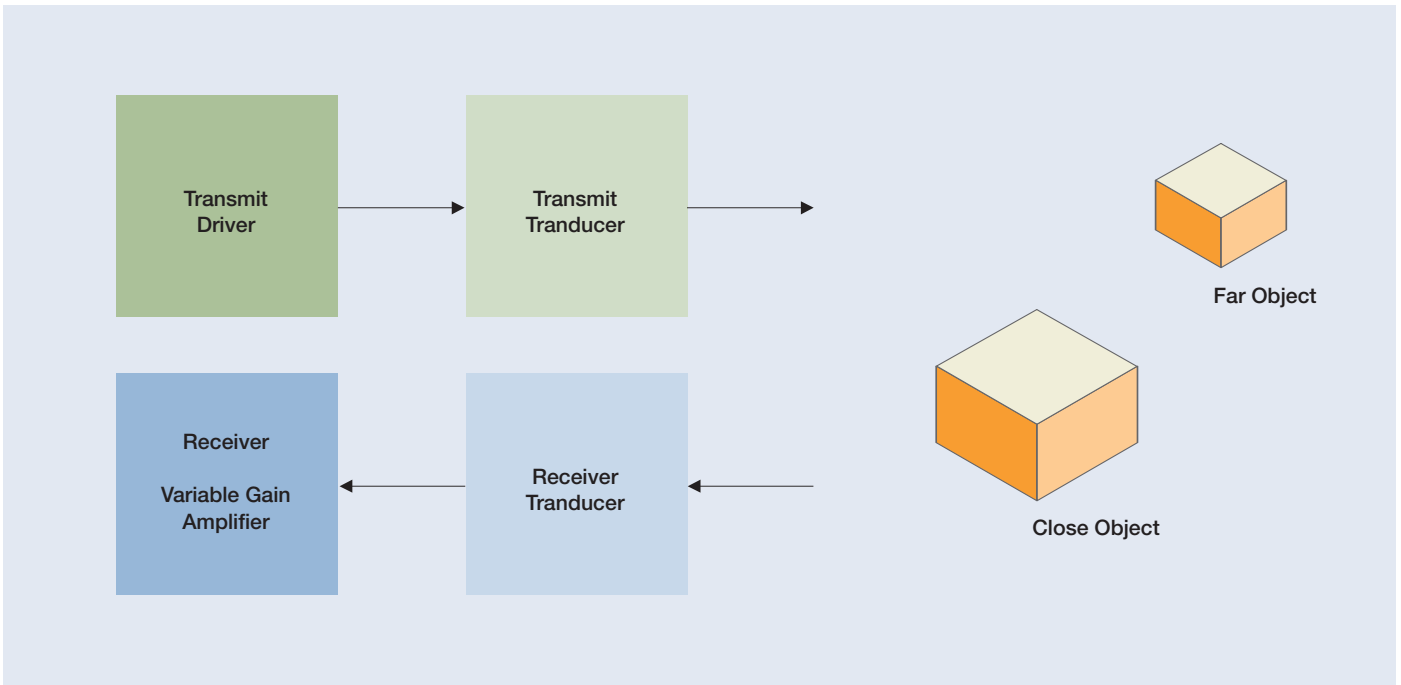


Figure 2.1. Block diagram of ultrasonic range detector.

Application 2. Ultrasonic Range Detector

In this example we will look at the operation of an ultrasonic system used to identify the distance of various objects from the detector. The challenge is to determine the best gain setting for distances closer to and farther from the detector. The detector will work best if the reflected signals are as large as possible with little or no clipping. We also want to confirm that the drive to the transmitting transducer is the correct voltage and frequency. Figure 2.1 shows a diagram of the system.

The receiver circuit consists of fixed and variable gain amplifiers because the return signal from the ultrasonic transducer has very low amplitude. Figure 2.2 shows the performance at a setting of the gain of the variable gain amplifier of 8. The detected signal shown in the Yellow analog trace labeled "RECEIVER" displays the signal that is presented for detection to the A/D converter in the microcontroller. The return signals from two targets are

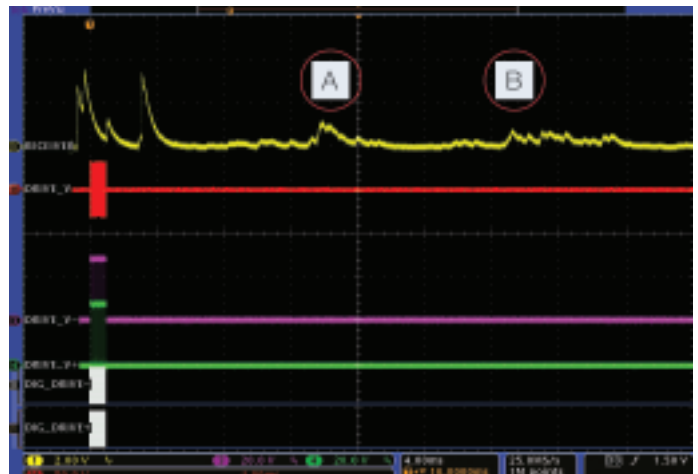


Figure 2.2. Transmitted and received signals with a gain of 8.

marked A and B. They are at about 14 and 24 milliseconds after the transmitted signal. Since sound travels at about 1 foot per second, and the sound needs to make a round trip from the transmitter to the receiver, the targets are at about 7 and 12 feet respectively.

The traces remaining in Figure 2.2 show the two-phase drive signals. The digital signals from the microcontroller are labeled “DIG_DRIVE-“ and “DIG_DRIVE+“. The analog voltages to the transducer are labeled “DRIVE_V-“ and “DRIVE_V+“. The difference of the voltages is shown in the red trace as “DRIVE_V”.

The reflected signals are visible on the RECEIVER trace, but are of very low amplitudes, so it appears that the gain is too low. The noise at the early part of the trace is due to signals mechanically coupling from the transmit transducer to the receive transducer. Since we are only interested in distances starting at about 2 feet (4 milliseconds), we can ignore these early signals.

We also need to confirm that the drive signal is correct. The drive signal needs to be about 1 millisecond in duration and at about 40 kHz. Both of these values can be confirmed by magnifying the trace in Figure 2.2. Figure 2.3 is the magnified trace showing the drive digital and analog signals. This figure shows the 1 millisecond duration of the pulse train and the correct frequency. Note that the digital drive and the resulting voltage waveform is a symmetric two phase signal as desired. The voltage drive in the combined signal “DRIVE_V” has a peak to peak value of about 60 volts as expected.

In Figure 2.4, the gain of the variable gain amplifier is increased by a factor of 2 to a total value of 16. With the higher gain setting, the signals are much larger. Note that the reflected signals are much larger than in Figure 2.2, but are still substantially below the clipping level of about 5 Volts.

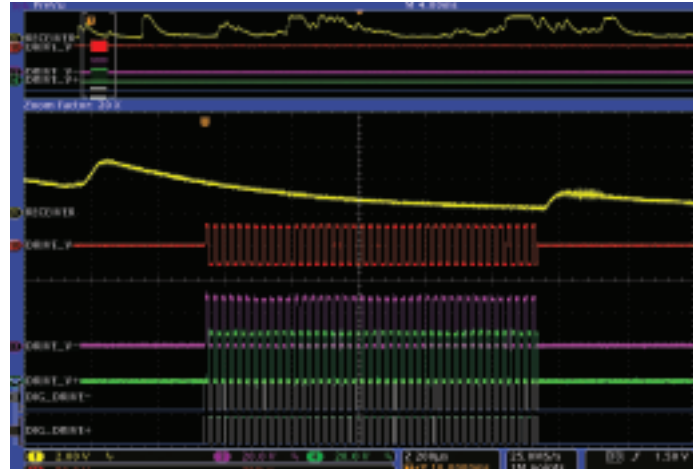


Figure 2.3. Transmitted signals magnified.

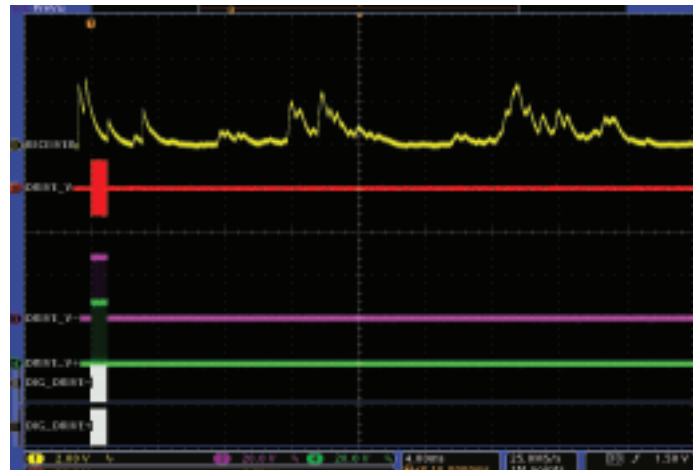


Figure 2.4. Transmitted and received signals with a gain of 16.

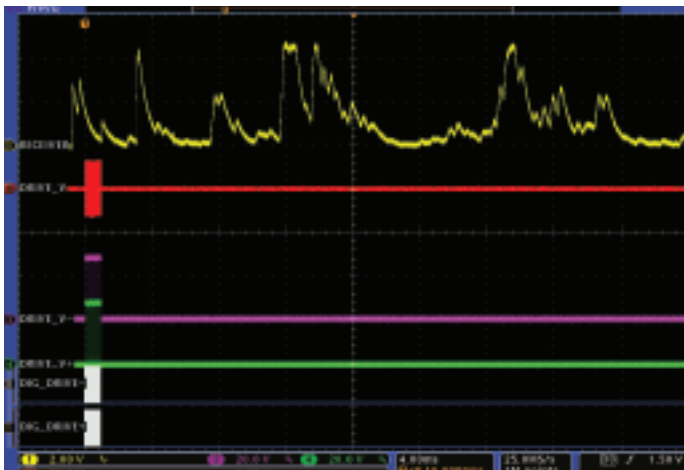


Figure 2.5. Transmitted and received signals with a gain of 32.

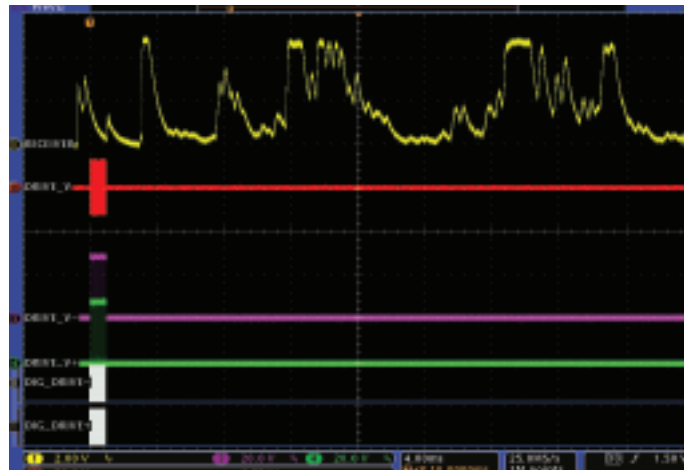


Figure 2.6. Transmitted and received signals with a gain of 64.

In Figure 2.5, the gain is again increased by another factor of 2 to a total of 32. Here we can see that the signal from the close target is starting to saturate the amplifier and clip, though the signal from the target that is farther away is near the full range of the amplifier at 5 Volts, but it is not clipping.

In Figure 2.6, the gain is further increased to 64. At this gain setting, the signals from both the near and the far targets are causing the amplifier to clip which reduces the accuracy of the distance reading. Clearly this gain setting is too high. Also note that there are multiple extraneous reflections showing on this trace which will make ranging more difficult.

In this example, we have used the deep memory of the oscilloscope to analyze the received signal of an ultrasonic distance measuring system to determine the appropriate gain setting of the drive signal. It appears that the best gain for this system is 32 because the measured signals are as large as possible with only a small amount of clipping. A finer adjustment of the fixed gain amplifiers could provide a slightly lower gain to provide the maximum usable signal without clipping. We were also able to verify that the drive signal is clean and of the correct timing, frequency and phase.

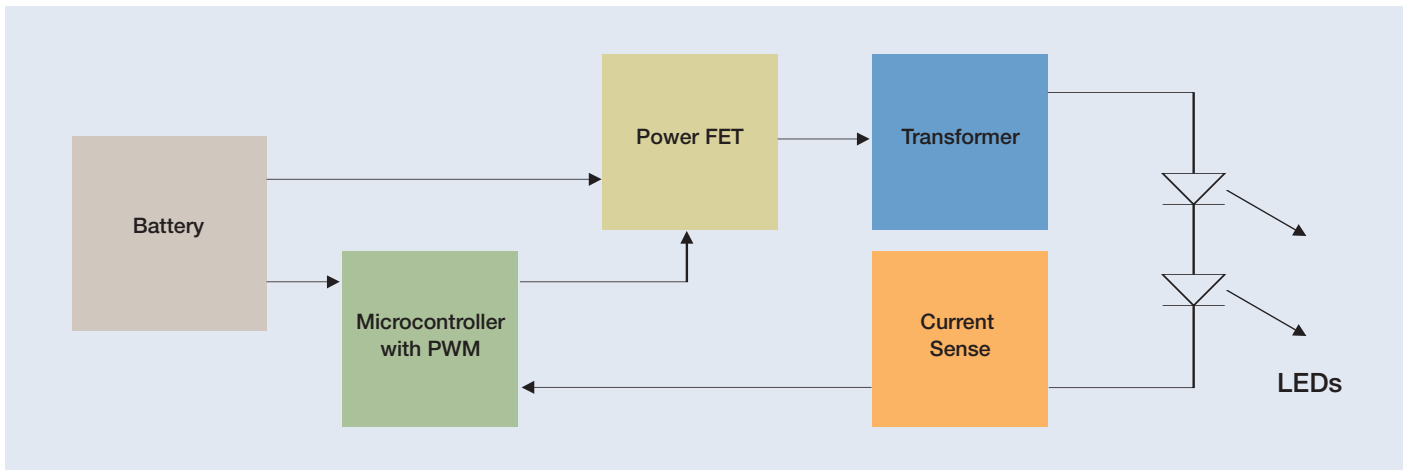


Figure 3.1. Block diagram of LED power system.

Application 3. High Brightness LED Power System

In this example we will look at the operation of the power supply electronics for driving high brightness LEDs. The challenge of this example is to assure that the drive current is stable despite gradual changes in the impedance of the LEDs as they heat up in normal operation, or as the battery voltage drops. The drive is based on a standard microcontroller pulse width modulated (PWM) controller. The LED current is measured by the microcontroller using an internal 8 bit A/D converter. The microcontroller incrementally adjusts the duty cycle to maintain the preset current. Because the current can only be adjusted in discrete increments of pulse width, there is the risk of noticeable flicker in the LEDs if the duty cycle changes back and forth between two states. Thus, some hysteresis must be introduced into the control loop to assure that there is no perceptible flicker. Figure 3.1 shows a block diagram of the system.

The power source is a battery, which could either be disposable or rechargeable. The battery provides power to the microcontroller and to the power circuit that controls the current to the LED. The microcontroller is programmed to control the duty cycle of the power transistor. A transformer is used because the battery voltage can be above or below the LED voltage depending on the state of charge of the battery and the temperature of the LEDs. In Figure 3.2, the green trace labeled “LED_I” shows the LED current measured at the LED with a current probe. The digital trace labeled “UPDATE” is a marker temporarily put in the microcontroller software to indicate when the microcontroller is updating the duty cycle of the power supply. The purple trace labeled “CUR@MICRO” is a filtered and amplified version of the LED current, which is fed to the A/D converter in the microcontroller to be compared with the programmed current value to make the pulse width adjustments. The yellow trace labeled “LED_V” is the voltage across the LEDs. The blue trace labeled “DRAIN_V” is the voltage at the drain (switching terminal) of the power transistor, which drives the transformer to power the LEDs. The digital signal labeled “DRIVE” is the drive to the gate of the power transistor.

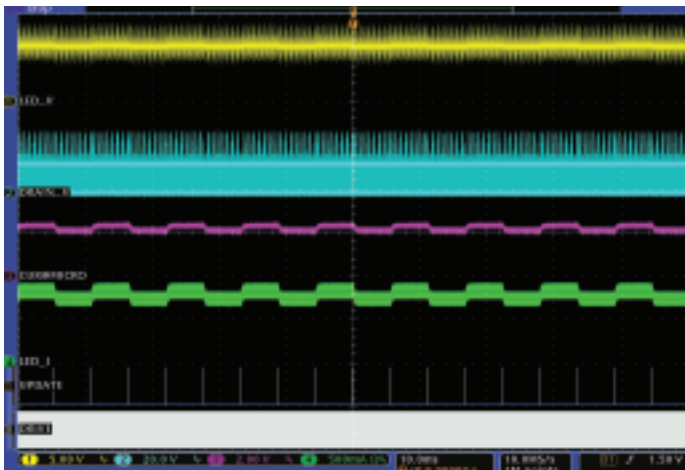


Figure 3.2. LED operation with current hysteresis value of 1.

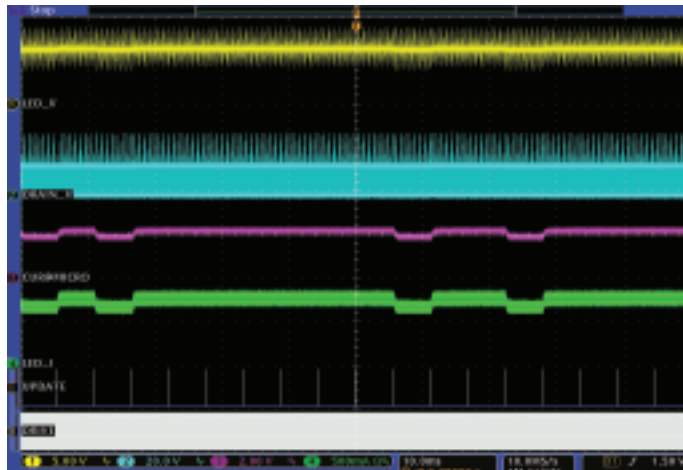


Figure 3.4. LED operation with current hysteresis value of 4.

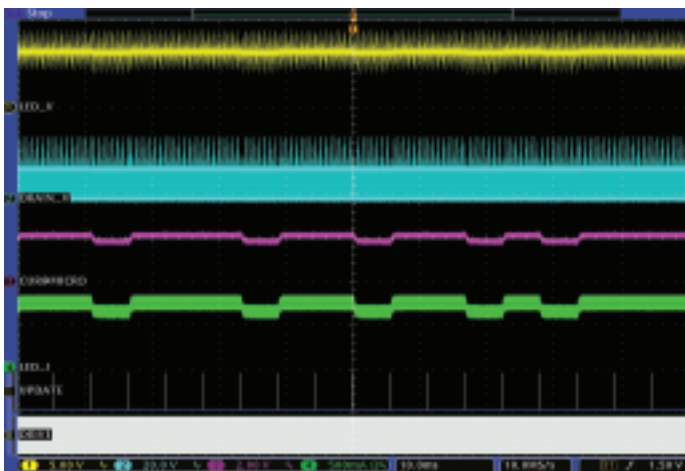


Figure 3.3. LED operation with current hysteresis value of 2.

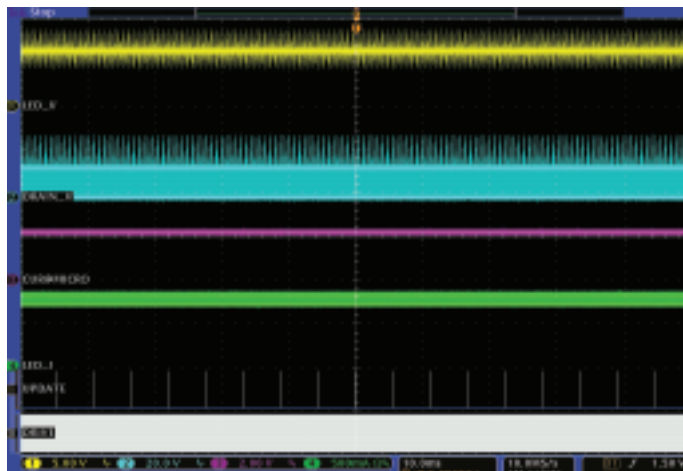


Figure 3.5. LED operation with current hysteresis value of 8.

In Figure 3.2, the hysteresis value is set to one, so that even a 1 bit change in the measured current signal will cause a change in the pulse width of the power drive signal. As can be seen, the pulse width and hence the current is changed each time the microcontroller software compares the measured current with the target value, as indicated by the markers. This results in the ripple current shown.

In Figure 3.3, the hysteresis value is changed to 2. There is still ripple on the current, but less, indicating that this is a better setting than in Figure 3.2.

In Figure 3.4, the hysteresis value is further increased to 4. As can be seen, there is less current ripple than in Figure 3.3, but this could still be objectionable.

Finally is Figure 3.5, the hysteresis value is increased to 8. The waveform shows no ripple at all. Thus, this is the best option.



Using Markers to Provide Visibility into Firmware Timing

Gaining visibility into firmware execution in microcontroller-based systems presents a challenge. For real-time control systems, the operation of the circuitry and of the microcontroller must be monitored when running at full speed. When microprocessors used external program memory, a logic analyzer could be used to track execution and measure timing. However, with on-chip program memory this approach is unfeasible. Today, almost all microcontrollers are supported by in-circuit debuggers and these tools typically have limited break points and limited, if any, real-time trace capability.

One useful technique to identify what the software in a microcontroller is doing is to toggle one or more I/O port pins at key points in the program execution. Often there are unused I/O port pins, or a port pin that is not used in the part of the code being debugged. The incremental cost of selecting a microcontroller with extra port pins to facilitate debugging is very small. A port pin can be toggled in various patterns to show different places in the code. For example, one, two, three or more consecutive pulses, or pulses of different widths can be used to mark different places in the code. While limited use of this technique is possible with just an analog oscilloscope, often the number of signals that must be monitored to debug or confirm the operation of the product exceeds the capability of conventional oscilloscopes and other traditional bench instruments. The Tektronix MSO4000 Series mixed signal oscilloscope is the ultimate all-in-one digital debug tool for embedded design.

Contact Tektronix:

ASEAN / Australasia (65) 6356 3900
Austria +41 52 675 3777
Balkan, Israel, South Africa and other ISE Countries +41 52 675 3777
Belgium 07 81 60166
Brazil & South America (11) 40669400
Canada 1 (800) 661-5625
Central East Europe, Ukraine and the Baltics +41 52 675 3777
Central Europe & Greece +41 52 675 3777
Denmark +45 80 88 1401
Finland +41 52 675 3777
France +33 (0) 1 69 86 81 81
Germany +49 (221) 94 77 400
Hong Kong (852) 2585-6688
India (91) 80-22275577
Italy +39 (02) 25086 1
Japan 81 (3) 6714-3010
Luxembourg +44 (0) 1344 392400
Mexico, Central America & Caribbean 52 (55) 5424700
Middle East, Asia and North Africa +41 52 675 3777
The Netherlands 090 02 021797
Norway 800 16098
People's Republic of China 86 (10) 6235 1230
Poland +41 52 675 3777
Portugal 80 08 12370
Republic of Korea 82 (2) 6917-5000
Russia & CIS +7 (495) 7484900
South Africa +27 11 206 8360
Spain (+34) 901 988 054
Sweden 020 08 80371
Switzerland +41 52 675 3777
Taiwan 886 (2) 2722-9622
United Kingdom & Eire +44 (0) 1344 392400
USA 1 (800) 426-2200

For other areas contact Tektronix, Inc. at: 1 (503) 627-7111
Updated 17 October 2007

For Further Information

Tektronix maintains a comprehensive, constantly expanding collection of application notes, technical briefs and other resources to help engineers working on the cutting edge of technology. Please visit www.tektronix.com



Copyright © 2007, Tektronix. All rights reserved. Tektronix products are covered by U.S. and foreign patents, issued and pending. Information in this publication supersedes that in all previously published material. Specification and price change privileges reserved. TEKTRONIX and TEK are registered trademarks of Tektronix, Inc. All other trade names referenced are the service marks, trademarks or registered trademarks of their respective companies.
11/07 DM 54W-21286-0

Tektronix[®]
Enabling Innovation



Paseo Imperial, 6 - 28005 Madrid
Tel.: 91 3654405 - Fax: 91 3654404
Email: afc@afc-ingenieros.com
Web: www.afc-ingenieros.com